Role of *YHM1*, encoding a mitochondrial carrier protein, in iron distribution of yeast

Emmanuel LESUISSE*, Elise R. LYVER†, Simon A. B. KNIGHT† and Andrew DANCIS†[1]

*Laboratoire d'Ingénierie des Protéines et Contrôle Métabolique, Institut Jacques Monod, Tour 43, Université Paris 7/Paris 6, 2 Place Jussieu, 75251 Paris cedex 05, France, and †Division of Hematology-Oncology, Department of Medicine, University of Pennsylvania, Philadelphia, PA 19104, U.S.A.

Mitochondrial carrier proteins are a large protein family, consisting of 35 members in *Saccharomyces cerevisiae*. Members of this protein family have been shown to transport varied substrates from cytoplasm to mitochondria or mitochondria to cytoplasm, although many family members do not have assigned substrates. We speculated whether one or more of these transporters will play a role in iron metabolism. Haploid yeast strains each deleted for a single mitochondrial carrier protein were analysed for alterations in iron homoeostasis. The strain deleted for *YHM1* was characterized by increased and misregulated surface ferric reductase and high-affinity ferrous transport activities. Siderophore uptake from different sources was also increased, and these effects were dependent on the *AFT1* iron sensor regulator. Mutants of *YHM1* converted into rho°, consistent with secondary mitochondrial DNA damage from mitochondrial iron accumulation. In fact, in the *Δyhm1* mutant, iron was found to accumulate in mitochondria. The accumulated iron showed decreased availability for haem synthesis, measured in isolated mitochondria using endogenously available metals and added porphyrins. The phenotypes of *Δyhm1* mutants indicate a role for this mitochondrial transporter in cellular iron homoeostasis.

Key words: carrier protein, haem, iron, mitochondria, *Saccharomyces*, yeast.

INTRODUCTION

Iron in cells exists primarily in complex with sulphur (Fe–S clusters) or in complex with porphyrin (haem). These critical cofactors mediate many of the myriad functions of iron proteins, including oxidation–reduction, electron transfer and oxygen binding [1]. Iron entering eukaryotic cells from the environment must travel to mitochondria, where haem [2,3] and Fe–S clusters [4] are made. Iron cofactors must reach proteins in various cellular compartments and, thus, the traffic of iron and iron cofactors into and out of mitochondria are critically important processes. However, molecular mediators for these processes are largely unidentified [4].

In an effort to identify genes that might be involved, we examined a collection of yeast mutants, each deleted for a single member of the mitochondrial carrier family [5]. The mutant collection was screened for abnormal regulation of cellular iron uptake. The rationale for this approach was derived from previous experience demonstrating effects of Fe–S cluster assembly mutants on cellular iron uptake. Mutants of Nfs1p [6,7], Ssq1p [8], Jac1p [9] and other components of the Fe–S cluster assembly machinery [4,10–12], all with principal mitochondrial localizations, were detected by associated increases in cellular ferric reductase and ferrous transport. These activities, involved in iron acquisition and usually repressed during growth in iron adequate media, were inappropriately expressed in Fe–S cluster assembly mutants. The misregulated activities were dependent on the Aft1p iron sensor regulator [6].

MCPs (mitochondrial carrier proteins) constitute a large protein family with 35 members encoded by the yeast nuclear genome [13]. Features of the protein family are integral membrane association and conserved sequence elements. Within cells, most of these proteins are found in the mitochondrial inner membrane. However, one family member is localized to the peroxisomal membrane [14]. Homologues of the yeast ATP/ADP translocators, which belong to this protein family, are found in hydrogenosomes (trichomonas) [15] and amyloplasts (maize) [16]. The topology of family members expressed in mitochondria is shared with the N- and C-termini of the nuclear-encoded polypeptides orientated towards the intermembrane space. The sequences include a tripartite structure consisting of three segments of 100 amino acids, each one containing two membrane-spanning domains and an intervening loop sequence. The proteins form homodimers and they function as exchangers or co-transporters at the mitochondrial inner membrane. A recent low-resolution crystal structure of the ATP/ADP carrier showed homodimerization and 3-fold symmetry in agreement with the 3-fold sequence repeats [17]. The substrates transported by carrier proteins of this family are extremely varied and include adenine nucleotides, phosphate, dicarboxylic acids, tricarboxylic acids, flavins, CoA, arginine-ornithine and pyruvate. The prototype protein for which most data exist is the ATP/ADP carrier. The substrates for particular MCPs were often identified by hints from the phenotypes of the corresponding yeast mutants. In some cases, the hints were straightforward, as in arginine auxotrophy caused by a defect in the arginine-ornithine transporter *ARG11* [18], and in other cases the hints were less straightforward, as for leucine auxotrophy associated with the CoA transporter *LEU5* [19]. A number of transporters have been studied by incorporation of purified proteins into liposome vesicles, which then reconstituted specific transport activities (e.g. Arg11p for ornithine). Recently, MCPs have been implicated in metal transport, although none has been studied yet by reconstitution. A carrier protein has been shown to mediate transport of iron into mitochondria [20,21] and delivery

Abbreviations used: BPS, bathophenanthroline disulphonic acid; DAPI, 4,6-diamidino-2-phenylindole; ENB, enterobactin; FCH, ferrichrome; FOB, ferrioxamine B; MCP, mitochondrial carrier protein; mtDNA, mitochondrial DNA; PP, protoporphyrin; TAF, triacetylfusarinine C; Zn-PP, zinc PP.

[1] To whom correspondence should be addressed (e-mail adancis@mail.med.upenn.edu).

of manganese to Sod2p in the mitochondrial matrix [22]. To date, more than half of the family members do not have substrates identified [13].

In the present study, we evaluated the regulated expression of ferric reductase and ferrous transport in a collection of yeast mutants, each deleted for a single MCP. We noted major effects of the deletion of *YHM1*. We observed further a rapid and preferential accumulation of iron in mitochondria of this mutant, suggesting that the carrier plays a role in cellular iron metabolism.

EXPERIMENTAL

Growth media

Rich media consisted of 1 % (w/v) yeast extract, 2 % (w/v) peptone, 100 μg/ml adenine and various carbon sources. In most experiments, 2 % (w/v) glucose was used as the carbon source (YPAD). In some experiments, cells were precultivated in 2 % (w/v) raffinose (YPAR) to induce mitochondrial biogenesis. For assessment of respiratory function, cells were grown on agar plates containing 3 % (v/v) ethanol as a non-fermentable carbon source (YE). The deletion strains were grown in YPAD with 200 μg/ml G418 added to the medium to select for the KAN cassette used in knockout construction [23]. For ferrous iron uptake and ferric reductase experiments, 50 μM copper sulphate was added to YPAD.

Yeast strains and crosses

The parental strains BY4741 and BY4742 were exposed to ethidium bromide to ablate mtDNA (mitochondrial DNA), creating BY4741 rho° and BY4742 rho° respectively [24]. The haploid MCP mutants in the BY4741 background were obtained from the EUROSCARF (European *Saccharomyces cerevisiae* Archive for Functional Analysis, Institut für Mikrobiologie, Johann Wolfgang Goethe-Universität, Frankfurt am Main, Germany) collection or from Invitrogen (Carlsbad, CA, U.S.A.). Assignment to the MCP family was as described by Belenkiy et al. [13]. The *Δleu5* strain was not available and was omitted from the screening. *RIM2* and *PET9* were listed as essential genes, and we therefore obtained the diploids and sporulated them. The *Δpet9* spore clones were non-viable, but *Δrim2* spore clones grew into small colonies and several clones were included in the screening. An *nfs1-14* strain was created by gene transplacement of a 5 kb *Bam*HI–*Eco*RI fragment containing the mutant allele and flanking *LEU2* gene into strain YPH499. Crosses of haploid strains were performed by micromanipulation of zygotes. Sporulation and tetrad dissection were performed according to published methods [25]. For creating the double *Δyhm1Δaft1* strain, a *URA3* cassette inserted into a unique *Hin*dIII site in the genome of strain CM3260Δaft1 [9] was amplified with flanking sequences and used to transform strain BY4741*Δyhm1* and control strains. The correctness of the integration was verified with PCR primers from outside the insertion site.

Biochemical assays

Ferric reductase and ferrous iron transport assays were performed as a combined microtitre plate assay. The controls and mutants were inoculated in triplicate in a 96-well plate in YPAD containing 50 μM copper sulphate. After growth for 16 h at 30 °C, the contents of each well were diluted 10-fold into fresh medium of the same composition, and the cells were allowed to reach exponential growth (4 h). The microtitre plates were cooled by floating in an ice-water bath, and the cells were washed free of medium by centrifuging and resuspending in ice-cold citrate buffer (50 mM sodium citrate, pH 6.5/5 % glucose). After several washes, the cells were resuspended in 100 μl of citrate buffer for measurement of turbidity (absorbance A at 720 nm). While setting up the assays, samples were maintained on ice. For ferric reductase, 90 μl of the cells were incubated with 1 mM ferric ammonium sulphate and 1 mM BPS (bathophenanthroline disulphonic acid) for 1 h at 30 °C, and the reaction was stopped by the addition of 50 % trichloroacetic acid. Cells were removed by centrifugation and the A_{515} of the ferrous iron–BPS complex was measured. For ferrous iron uptake, 10 μl of cells were added to the 90 μl of iron labelling solution consisting of 1 μM ^{55}Fe (50 Ci/g; Amersham Biosciences, Piscataway, NJ, U.S.A.), 1 mM sodium ascorbate and 50 mM sodium citrate. The uptake was allowed to proceed for 1 h at 30 °C and was terminated by harvesting the cells on 96-well glass-fibre filters, using a Wallac cell harvester. The cells retained on the filter were washed free of unincorporated iron with water, dried and soaked in a liquid-scintillation fluid (Betalplate Scint; Wallac, PerkinElmer Life Sciences, Boston, MA, U.S.A.). The radioactivity was measured by scintillation counting (Wallac 1450 Microbeta). Results are reported as c.p.m. $\cdot$ $(10^6$ cells$)^{-1} \cdot h^{-1}$. A similar assay was performed for measuring cellular iron uptake from radiolabelled siderophores; in this experiment, radioactivity retained on filters was measured in the presence of a solid sheet of scintillant (MeltiLex, Wallac). The mesylate derivative of FOB (ferrioxamine B; Desferal, Novartis) was radiolabelled, and FCH (ferrichrome), TAF (triacetylfusarinine C) and ENB (enterobactin) were purchased from Biophore Research Products (Tubingen, Germany) and radiolabelled [26]. Aconitase was assayed by measuring the formation of *cis*-aconitate at 240 nm as described in [27]. Succinate dehydrogenase was measured as described in [28]. Cells for the isopropylmalate isomerase (Leu1p) activity assay were grown in the defined medium and lysates were made by vortex-mixing of cells in a microcentrifuge tube to which glass beads were added. Protein concentration was determined by measurement with bicinchoninic acid (Pierce, Rockford, IL, U.S.A.). The substrate citraconic acid was purchased from Aldrich and pH was adjusted to 7.0 with sodium hydroxide. Substrate was added at 4 mM and the rate of decline of A_{235} was observed. Activity reflecting disappearance of citraconate substrate was expressed in terms of μmol $\cdot$ min^{-1} $\cdot$ (mg of protein)$^{-1}$ or units. Details of the assay have been described by Kohlhaw [29].

Antibodies

The open reading frame for Isu1p was cloned into pET21b and expressed in *Escherichia coli* BL21(DE3) codon plus. Protein was purified using a His_6 tag, and rabbits were injected for the generation of polyclonal antibodies directed against Isu1p. Antibodies to Aco1p [12], Ssq1p [9], Yfh1p [30] and Nfs1p [6] have been described previously. Rabbit polyclonal antibody against Ccp1p was a gift from Dr Debkumar Pain (Department of Pharmacology and Physiology, UMDNJ-New Jersey Medical School, Newark, NJ, U.S.A.). Mouse monoclonal antibodies against porin, Por1p (mitochondria), Pgk1p (cytoplasm), Dpm1p (endoplasmic reticulum) and Cpy1p (vacuole) were purchased from Molecular Probes (Eugene, OR, U.S.A.).

Radiolabelling of yeast cells with ^{55}Fe and cell fractionation

Cells were grown in rich media (YPAD) to A_{600} 1.0. At this time, ^{55}Fe (200 nM final, 50 Ci/g) was added directly to the medium containing growing cells. Cultures were returned to the incubator during the 1 h of labelling. The cultures were then cooled in an ice-water bath, harvested and washed several

times with sodium citrate buffer (50 mM, pH 6.5) to remove any unincorporated counts. The wash buffer was tested and contained negligible radioactivity. Before cell fractionation, an aliquot of washed cells was removed for scintillation counting in a Beckman LS6500 with ScintiSafe Econo 1 LSC Cocktail (Fisher Scientific, Pittsburgh, PA, U.S.A.). Cell-wall digestion was performed for 20 min with Zymolyase 100T. A crude mitochondrial fraction was isolated as described in [31] after douncing with 15 strokes while on ice. The post-mitochondrial fraction was centrifuged at 100 000 ***g*** for 20 min. The supernatant following centrifugation was analysed as the cytoplasmic fraction. Mitochondria were purified further as follows. A portion of mitochondria, equivalent to 5 mg of protein, was layered on top of a step gradient consisting of 2 ml of 40 % (v/v) Percoll in 50 mm Tris/HCl (pH 7.5), 0.6 M sorbitol and 8 ml of 20 % Percoll in the same buffer. Gradients were centrifuged at 105 000 ***g*** in a Beckman Sw41 Ti swinging bucket rotor for 30 min at 4 °C. The mitochondria were collected from the 20–40 % interface with a Pasteur pipette and washed three times in 15 ml of mitochondrial isolation buffer to remove the Percoll. A portion of the mitochondria and cytoplasm fractions were suspended in 50 mm Tris/HCl (pH 7.5), 0.6 % SDS and analysed for iron content by scintillation counting and for protein content by bicinchoninic acid assay (Pierce). The purified mitochondrial fractions were reactive with antibodies to mitochondrial proteins, but non-reactive with antibodies to vacuolar (anti-Cpy1p), cytoplasmic (anti-Pgk1p) or endoplasmic reticulum (anti-Dpm1p) marker proteins.

Iron release from mitochondrial lysate

Isolated mitochondria were lysed in 0.6 M sorbitol, 10 mM Tris/HCl (pH 7.4) and 0.1 % Tween 80. After lysis, 5 mM sodium ascorbate and 200 μM BPS were added. A_{535} was measured at 25 °C over time and the concentration of the ferrous iron–BPS complex was calculated.

Haem synthesis in intact isolated mitochondria

Isolated mitochondria (0.2 mg of protein/ml) in 0.6 M sorbitol with 50 mM Tris/HCl (pH 7.4), with or without 10 mM EDTA, and no added metals were examined. The reaction was initiated by adding 2 μM protoporphyrinogen. PP (protoporphyrin IX, excitation at 410 nm and emission at 632 nm) or Zn-PP (zinc-PPIX, excitation at 420 nm and emission at 587 nm) formation was studied continuously by their fluorescent emissions. Haem formation was calculated as PPIX formed in the presence of EDTA minus PPIX and Zn-PPIX formed in the absence of EDTA [32]. Protoporphyrinogen was prepared from PP by reduction with a sodium amalgam [33].

Microscopy

Strains were grown for 6 days on YPAR agar plates. Cells were fixed in 70 % ethanol, washed and resuspended in PBS. DNA was stained by adding 0.2 μg/ml DAPI (4,6-diamidino-2-phenylindole) and the cells were attached to polylysine-treated slides and mounted with Fluoromount-G (Southern Biotechnology Associates, Birmingham, AL, U.S.A.). Cells were viewed with a Nikon Eclipse E800 microscope with a $\times$ 60 objective and $\times$ 2.5 magnifier tube. Images were recorded with Hamatsu C4742 digital camera and Image-Pro Plus software.

Other methods

SDS/PAGE, immunoblotting and signal development using ECL® (Amersham Biosciences) were performed according to standard methods.

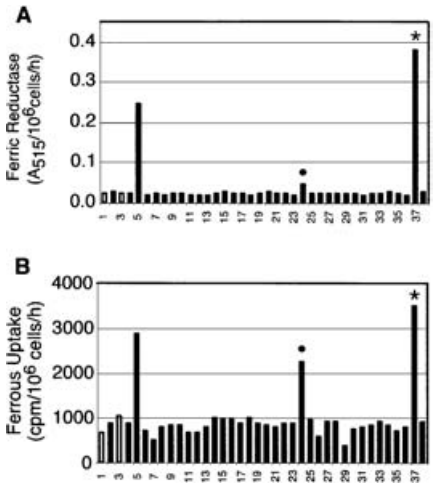

Figure 1 Screen of MCP mutants for iron regulatory phenotypes

Yeast strains (column no. in parentheses) BY4741 (1), BY4741 rho° (2), BY4742 (3), BY4742 rho° (4), *nfs1-14/LEU2* (5), YJR077C *Δmir1* (6), YMR056C *Δaac1* (7), YBR085W *Δaac3* (8), YOR130C *Δarg11* (9), YOR100C *Δcac/Δcrc1* (10), YBR291C *Δctp1* (11), YJR095W *Δacr1* (12), YKL120W *Δoac1/Δpmt1* (13), YLR348C *Δdic1* (14), YIL134W *Δflx1* (15), YMR241W (16), YPR011C (17), YNL083W *Δyng2* (18), YGR096W (19), YOR222W (20), YPL134C *Δodc1* (21), YPR058W *Δymc1* (22), YBR104W *Δymc2* (23), YJL133W *Δmrs3* (24), YKR052C *Δmrs4* (25), YNL003C *Δpet8* (26), YEL006W (27), YIL006W (28), YBR192W *Δrim2* (29), YPR128C (30), YER053C (31), YFR045W (32), YPR021C (33), YMR166C (34), YGR257C (35), YDL119C (36), YDL198C *Δyhm1* (37) and YDR470C *Δugo1* (38) were grown at 30 °C in YPAD with 50 μM copper sulphate before measuring ferric reductase (**A**) and ferrous iron uptake (**B**). Strains 1–5 represent controls. Strains 6–38 are MCP mutants in the order presented in [13]. *Δmrs3* (24) is shown with a (●) and *Δyhm1* (37) is shown with a (*) above the corresponding bar graphs. Results are medians for triplicate measurements. For reductase measurements, S.D. < 15 % with the exception of *Δrim2* (29), which showed a 42 % S.D. For ferrous uptake measurements, S.D. < 15 % with the exception of *Δrim2* (29), which again showed a 42 % S.D., YER053C (31), showed a 19 % S.D. and *Δugo1* (38), showed a 17 % S.D.

RESULTS

Haploid yeast strains, each deleted for a single MCP, were obtained from the yeast genome deletion collection [5]. Of the 35 predicted MCPs encoded in the yeast genome, we were able to obtain haploid deletion strains for 33. The *Δleu5* knockout was unavailable and the *Δpet9* knockout was non-viable. *RIM2* was listed as an essential gene. However, when the diploid knockout for *RIM2* was sporulated, tetrad clones carrying the deletion were found to be viable albeit slow growing, and these were included in the screening assays. The parental strains, BY4741 and BY4742, were included as controls, as were congenic rho° strains made by ethidium bromide treatment. Also, a strain with the *nfs1-14* allele transplaced into the genome was included as a control. *NFS1* encodes a cysteine desulphurase with a primarily mitochondrial localization, and the *nfs1-14* mutation is associated with increased cellular ferric reductase and ferrous iron uptake activities [6].

We previously found that mutants with altered iron distribution between mitochondria and cytoplasm exhibit abnormal increases in these activities [8]. Therefore the yeast MCP mutants and control yeast strains were analysed for cell-surface ferric reductase and high-affinity ferrous transport. These are independent measurements of regulated activities, which in the normal cell are homoeostatically regulated in response to iron availability. In the screening assays (Figure 1), wild-type strains of both mating types and rho° isolates showed similar low levels of ferric reductase and ferrous transport. Marked increases in ferric reductase and ferrous transport were observed in the *Δyhm1* (YDL198C) mutant, and these activities were similar to levels observed in the *nfs1-14*

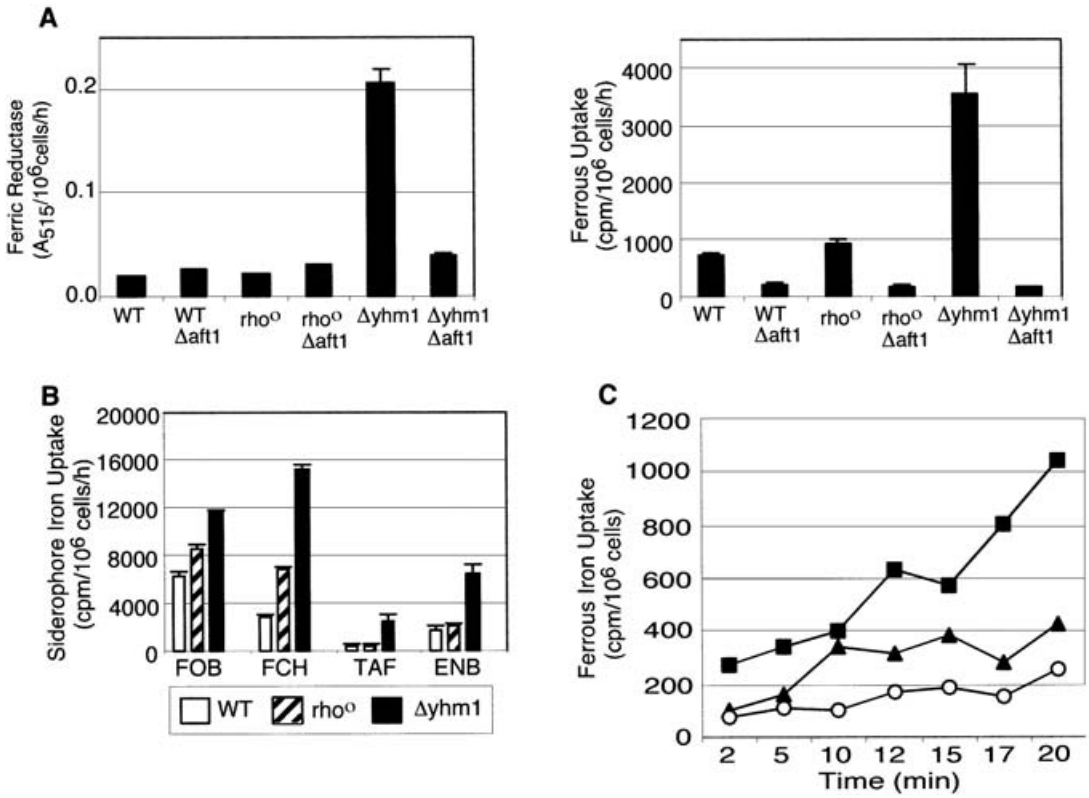

Figure 2 Iron uptake misregulation as a consequence of *Δyhm1* mutation

(**A**) Ferric reductase and ferrous uptake induction in *Δyhm1* depends on *AFT1*. Wild-type BY4741, congenic rho° and *Δyhm1* strains were transformed with a cassette to interrupt *AFT1*. The single and double mutants were tested for ferric reductase and ferrous transport. Assays were performed in triplicate and mean was calculated. S.D. are shown by error bars. (**B**) Iron uptake from siderophores is increased in *Δyhm1* mutant. The cells were grown in raffinose-based medium and were transferred to glucose medium (YPAD) for 5 h. The cells were washed and suspended at high density (A_{600} 10) in the presence of 1 μM of different ^{55}Fe-labelled iron chelates, FOB, FCH, TAF and ENB. Iron uptake proceeded for 30 min at 30 °C, and cells were filtered and the cell-associated radioactivity was determined by scintillation counting. Assays were performed in triplicate and the mean was calculated. S.D. are shown by error bars. (**C**) Time course of ferrous iron uptake. Cells were grown to exponential phase in YPAD, washed free of medium and resuspended in ice-cold citrate buffer at A_{600} 2.0. The samples were warmed to 30 °C for 5 min before the addition of an equal volume of prewarmed solution of ^{55}Fe ferrous citrate such that the final iron concentration for the assay was 1 μM. Aliquots were removed at various time points and placed in an ice-water bath to stop the iron uptake. Cells were harvested by filtration on glass fibre filters and the amount of radioactivity was measured by scintillation counting as described previously [48]. The time course represents a single experiment. ■, *Δyhm1*; ▲, rho°; ○, WT.

mutant (Figure 1). The *Δmrs3* (YJL133W) deletion was also clearly abnormal. Ferrous uptake activity was increased compared with the parental strains, and ferric reductase was also increased. Similar effects were not observed in the mutant deleted for the homologous gene *Δmrs4* (YKR052C) (Figure 1). *MRS3* and *MRS4* have previously been linked to iron metabolism [20,21]. *YHM1* was previously identified as a high copy suppressor of mtDNA instability associated with an *ABF2* deletion, but *YHM1* has not been previously associated with iron metabolism [34].

The markedly increased ferric reductase and ferrous transport activities associated with the *Δyhm1* mutation were evaluated further. The *Δyhm1* strain was crossed with the parental strain of opposite mating type and the diploid was sporulated. The heterozygote had no detectable phenotype, indicating that the iron regulatory phenotype was recessive. Products of four individual meioses were dissected and analysed. The clones carrying the *Δyhm1::KAN* knockout were identified by their G418 resistance. The segregants exhibited increased ferric reductase and ferrous transport activities in 2+:2− pattern consistent with a nuclear gene effect.

We speculated whether the perturbed iron uptake in the mutant was mediated by *AFT1*. *AFT1* encodes a major iron sensor regulator of yeast, responsible for regulating expression of high-affinity iron uptake in response to environmental iron signals [35]. Therefore a double-mutant strain was constructed lacking both *YHM1* and *AFT1*. This double mutant showed ferric reductase and ferrous transport activities that were no longer increased compared with the wild-type control strain (Figure 2A). Thus the effect of the *Δyhm1* deletion on cellular iron uptake was entirely dependent on the presence of an intact copy of *AFT1*.

Ferric reductase and ferrous transport activities vary in response to iron levels through control of *AFT1* and its paralogue *AFT2* [36,37]. Iron uptake from siderophores occurs by a separate pathway, also under *AFT1*/*AFT2* control, mediated by four distinct transporters [38–40]. This non-reductive pathway was induced in the *Δyhm1* mutant as reflected by increased iron uptake from different siderophores. Iron uptake in the mutant was increased from FOB, FCH, TAF and ENB, indicating activation of distinct siderophore transporters (Figure 2B). In some cases, i.e. for FOB and FCH, increased iron transport activities were seen in the congenic rho° strain compared with the rho$^+$ control. However, the *Δyhm1* mutant showed still higher activities for each of these transport substrates. Induction of cellular iron uptake activities in the *Δyhm1* mutant thus affected both reductive and non-reductive iron sources, consistent with a general activation of *AFT1*/*AFT2* target genes.

These measurements showing increased iron accumulation from various sources at 1 h suggested that the *Δyhm1* mutant

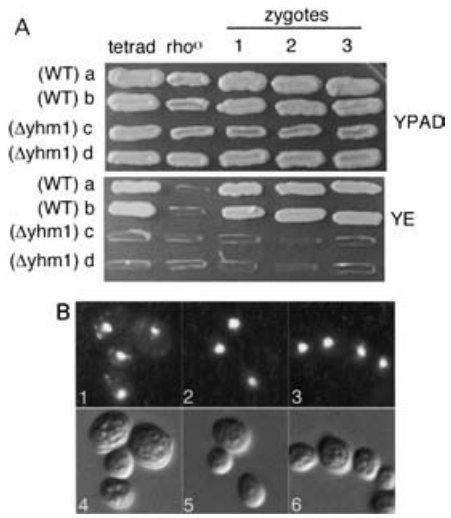

Figure 3 Nuclear mutation of *YHM1* (*Δyhm1*) associated with loss of mtDNA

(**A**) Genetic evidence of mtDNA damage. A backcross of the *Δyhm1* mutant with a parental strain of opposite mating type, BY4742, was sporulated and *Δyhm1* clones were identified by G418 resistance conferred by the knockout cassette. Each of four tetrad clones from a single meiosis was crossed with rho° testers of opposite mating type. Three zygotes from each cross were manipulated and analysed for growth on YE (ethanol) or YPAD (glucose). Failure of the zygotes to grow on ethanol plates is diagnostic of mtDNA inactivation (see tetrads c and d, zygotes 1, 2 and 3). (**B**) Microscopic evidence of mtDNA loss. Wild-type (squares 1 and 4), *Δyhm1* (squares 2 and 5) and rho° (squares 3 and 6) were grown for 6 days on YPAR agar plates. Cells were stained with DAPI and viewed under UV light to visualize DNA (squares 1–3) and differential interference contrast to show cell morphology (squares 4–6).

might exhibit an increased rate of cellular iron uptake. A time-course experiment was performed to evaluate more directly iron uptake rates. The mutant and control strains were grown to exponential phase, washed free of medium and temperature-shift was used to start and stop iron uptake from ferrous citrate. Cells were shifted from 4 to 30 °C and mixed with warmed buffer containing radioactive iron. Samples were then removed at intervals, cooled in an ice-water bath and subsequently tested for cell-associated radioactivity. Despite growth on iron adequate medium, *Δyhm1* mutants manifested greatly increased rates of iron uptake compared with parental or rho° controls (Figure 2C).

The *Δyhm1* mutant strain appeared de-pigmented and did not grow on non-fermentable carbon sources even after prolonged incubation. These phenotypes often denote loss or damage to mtDNA. The parental mutant (results not shown) and tetrad clones derived from a backcross with a wild-type strain were assessed using a genetic method to evaluate mtDNA function. The tetrad clones were mated with rho° tester strains completely lacking in mtDNA. Zygotes were manipulated and allowed to grow into colonies and these were tested for their ability to grow on ethanol-based medium (YE), a phenotype that requires mtDNA function. The zygotes formed by crossing of WT (wild-type) with the rho° testers grew well (Figure 3A, rows a and b), whereas the zygotes formed by crossing of mutant (*Δyhm1*) clones with the rho° testers (Figure 3A, rows c and d) did not grow on YE medium. These results show that the *Δyhm1* mutants had undergone mtDNA damage or loss. To distinguish these possibilities, we directly examined the mutant cells for the presence of mtDNA by DAPI staining (Figure 3B). The wild-type (Figure 3B, square 1) showed punctate staining near the cell periphery indicative of mtDNA, whereas *Δyhm1* (square 2) and rho° control (square 3) showed no cytoplasmic staining. Nuclear DNA was stained in all three strains. Thus the *Δyhm1* mutant was in fact rho°. Furthermore, the fact that the phenotype recurred in the mutant tetrads following a backcross showed that the effect was a consequence of the nuclear mutation. Iron accumulation in mitochondria has been shown to mediate mtDNA damage in some mutants lacking critical components for Fe–S cluster synthesis. Therefore we considered that the *Δyhm1* mutant might be accumulating mitochondrial iron.

Cellular iron distribution was tested in wild-type, rho° and *Δyhm1* strains following a pulse of radioactive iron. A rho° control was included because *Δyhm1* mutants were rho°. Strains were grown to exponential phase in YPAD, and radioactive iron was added directly to the growing culture as a tracer for 1 h. After washing to remove unincorporated counts, radioactivity was assessed in whole cells. Subsequently, the cells were separated into cytoplasmic and pure mitochondrial subcellular fractions for measurement of radioactive iron and protein concentration. As observed previously, whole cell radioactive iron was increased in the *Δyhm1* mutant compared with the controls (Figure 4A). Cytoplasmic iron in the *Δyhm1* mutant was only slightly increased (1.3-fold) compared with the rho° strain (Figure 4B). In contrast, mitochondrial iron in the *Δyhm1* mutant was increased 26-fold (Figure 4C). The increase in mitochondria was out of proportion to the increase in total cellular iron (Figure 4D).

The maldistribution of cellular iron observed following a short pulse of radioactive iron was also observed at steady state (24.5 nmol iron/mg of mitochondrial protein in the mutant compared with 2.1 nmol/mg in the wild-type). The characteristics of mitochondrial iron accumulating in the mutant were examined. When mitochondrial lysates from wild-type and mutant were exposed directly to the ferrous iron chelator BPS, no coloured ferrous complex appeared indicating that ferrous iron was not present or was not accessible to the chelator. After addition of ascorbic acid as a reductant, the coloured ferrous iron–BPS complex appeared over time (Figure 5), indicating progressive reduction and mobilization of mitochondrial ferric iron species. The signal was markedly increased in the mutant, consistent with the increased amount of iron in the mutant mitochondria. A rho° control was indistinguishable from wild-type (results not shown).

In some respects, the *Δyhm1* mutant appeared to phenocopy mutants involved in Fe–S cluster synthesis, exhibiting increased iron uptake and iron accumulation in mitochondria. Therefore we tested the status of cellular Fe–S cluster proteins in the *Δyhm1* mutant. The results did not support a generalized or a severe compartmental defect in Fe–S cluster proteins. The mutant had a marked decrease in aconitase, and activities were 98, 178 and 30 nmol of *cis*-aconitate formed · (mg of mitochondrial protein)$^{-1}$ · min^{-1} for wild-type, rho° and *Δyhm1* respectively. In contrast, succinate dehydrogenase, an Fe–S and haem-containing complex of the mitochondrial inner membrane, was not decreased in the mutant. Levels were 2.6, 0.78 and 1.7 nmol of reduced *p*-iodonitrotetrazolium violet substrate formed · (mg of mitochondrial protein)$^{-1}$ · min^{-1} for wild-type, rho° and *Δyhm1* respectively. Isopropylmalate isomerase or Leu1p activity in a cytoplasmic lysate was decreased to 45 % compared with the rho° control. The measured activities were 0.21, 0.076 and 0.035 μmol · min^{-1} · (mg of protein)$^{-1}$ for wild-type, rho° and *Δyhm1* respectively [29].

We wanted to test the nature of iron accumulating in the mutant mitochondria, and to do this haem synthesis from endogenous metals was measured in isolated wild-type and mutant mitochondria. In this experiment (Figure 6), isolated mitochondria were exposed to protoporphyrinogen, allowing for *in situ* formation of the fluorescent PPIX intermediate. In the presence of metal chelator, the final step of haem synthesis (PPIX to

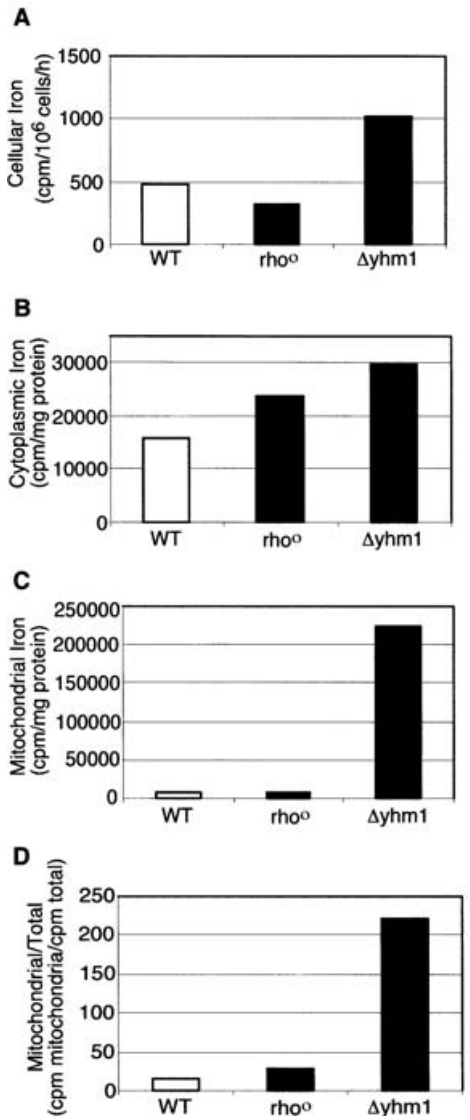

Figure 4 Iron distribution in *Δyhm1* mutants following a 1 h pulse with ^{55}Fe

Growing cells (WT, rho° and *Δyhm1*) in glucose media (YPAD) were labelled for 1 h with a trace amount of radioactive iron. Unincorporated iron was removed by washing and uptake of cellular iron was determined by scintillation counting. Cell fractionation was performed and purified mitochondrial and cytoplasmic fractions were isolated. Fe radioactivity in the fractions and protein content were measured. (**A**) Cellular iron levels. Whole cell radioactivity was measured before all manipulations involved in fractionation and is reported as c.p.m. · $(10^6$ cells$)^{-1}$ · h^{-1}. (**B**) Cytoplasmic iron levels. Following isolation of the post-mitochondrial supernatant, this fraction was centrifuged at 100 000 ***g*** for 20 min at 4 °C, and the supernatant was analysed for radioactivity and protein content. Results are reported as c.p.m./mg of cytoplasmic protein. (**C**) Mitochondrial iron levels. Mitochondria were purified on a Percoll step gradient. Fe radioactivity and protein concentration were determined. Results are c.p.m./mg of mitochondrial protein. (**D**) Ratio of mitochondrial iron to total cellular iron. Results are presented for a single representative experiment.

haem) was prevented by lack of metal availability, and fluorescent PPIX accumulated (Figure 6A) although at a slightly lesser rate in the mutant when compared with that in the wild-type. In the absence of chelator, PPIX was converted into haem or Zn-PPIX using endogenous metals. Under these conditions, PPIX was formed at similar rates in wild-type and mutant mitochondria (Figure 6B), and yet Zn-PPIX (Figure 6C) and haem (Figure 6D) were formed more slowly in the *Δyhm1* mutant. A parallel

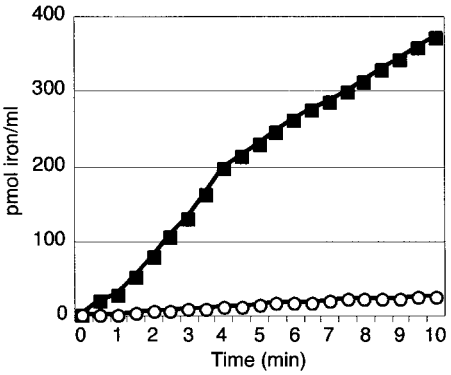

Figure 5 Steady-state iron accumulating in mitochondria of *Δyhm1* mutant

Wild-type and *Δyhm1* strains were grown in YPAD and mitochondria were isolated. Following solubilization in 0.1 % Tween 80 detergent, 5 mM sodium ascorbate and 200 μM BPS were added. The increase in A_{535} reflecting formation of a ferrous iron-bathophenanthroline complex was monitored over time. ■, *Δyhm1*; ○, WT. The data are from a single experiment.

experiment performed with the rho° strain showed no difference from the wild-type control (results not shown). We considered that deficiency in haem synthetic activity in the *Δyhm1* mutant might be owing to deficiency of ferrochelatase. However, this was ruled out, because ferrochelatase activity measured with added ferrous ascorbate, protoporphyrinogen and mitochondrial lysate was indistinguishable from wild-type activity. Thus the decrease in haem synthesis indicated that the large amount of accumulated iron in the *Δyhm1* mutant was unavailable for haem synthesis.

Protein levels in wild-type, rho° and *Δyhm1* mutant mitochondria were examined by immunoblotting of isolated mitochondria with selected antibodies. As a control, we performed blotting with antibody to the outer-membrane protein porin, and porin levels were indistinguishable in the three strains (Figure 7). Ccp1p, cytochrome *c* peroxidase, a haem protein of the intermembrane space [41], was decreased in the *Δyhm1* mutant. Aco1p and aconitase were also decreased consistent with lower aconitase activity of the mutant. In contrast, aconitase activity and Aco1p protein were increased in the rho° control compared with the wild-type. Proteins involved in Fe–S cluster assembly [4] were tested for their abundance by immunoblotting. Isu1p, a scaffold protein involved in assembling Fe–S cluster intermediates [10], was increased in *Δyhm1* when compared with the wild-type, although a similar increase was observed for the rho° control. Yfh1p, the yeast frataxin homologue, was decreased when compared with wild-type and rho° controls. Levels for Nfs1p (cysteine desulphurase) and Ssq1p (chaperone protein), were unchanged in the *Δyhm1* strain. Low-temperature spectra of whole cells showed deficiencies of *b* and *c* type cytochromes in the *Δyhm1* mutant and rho° strain that were similar in degree (Figure 8).

DISCUSSION

Iron uptake systems have been characterized, which function at the cell surface [42]. Fe–S cluster forming [43] and haem synthesis [3] activities have been characterized in mitochondria. However, iron transport and transfer processes, which link these two areas of the cell have not been defined. In the present study, we screened MCP mutants for effects on iron homoeostasis.

MCPs are a large family of proteins including 35 members in *S. cerevisiae*, which are localized in yeast. They have been found in the mitochondrial inner membrane although one exceptional family member was found in peroxisomal membranes [13].

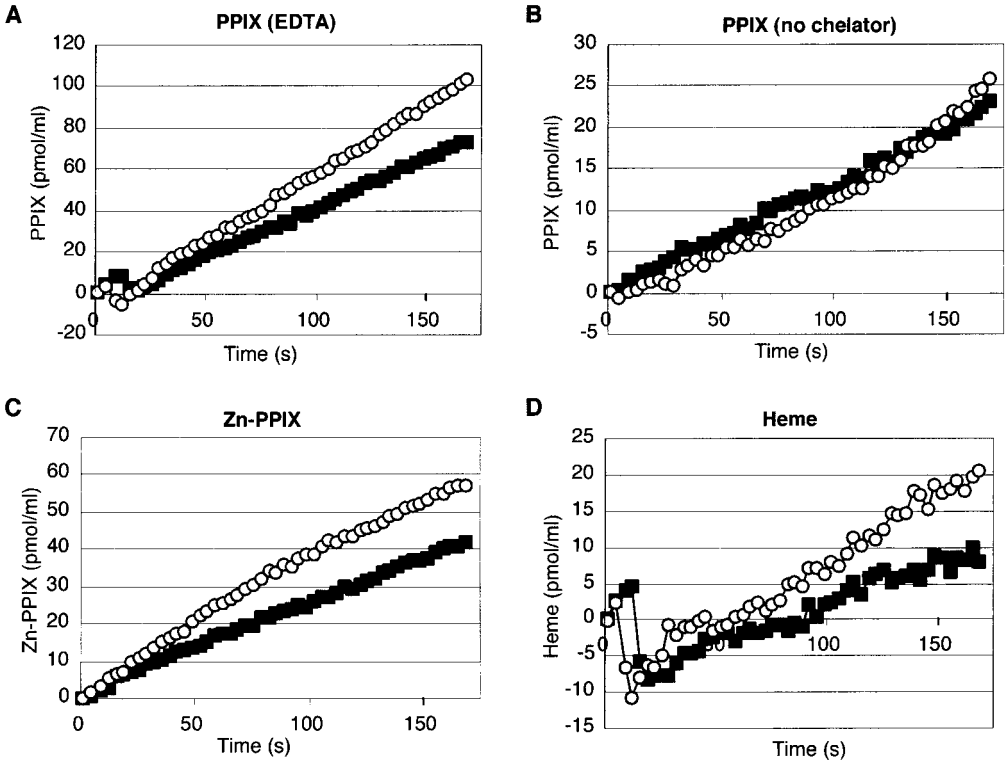

Figure 6 Haem synthesis from endogenous metals is decreased in isolated mitochondria of *Δyhm1* cells

Mitochondria were isolated from wild-type and *Δyhm1* mutants grown in glucose medium. Isolated mitochondria (0.2 mg of protein/ml) were suspended in buffer consisting of 0.6 M sorbitol with 50 mM Tris/HCl (pH 7.4), with (**A**) or without (**B**–**D**) 10 mM EDTA. No metals were added. The reactions were initiated by adding 2 μM protoporphyrinogen to the suspended mitochondria. Fluorescence from the formation of PPIX, excitation at 410 nm and emission at 632 nm (**A**, **B**) or Zn–PPIX, excitation at 420 nm and emission at 587 nm (**C**) were followed continuously. Haem formation was calculated as PPIX formed in the presence of EDTA minus PPIX + Zn-PPIX formed in the absence of EDTA (**D**). ■, *Δyhm1*; ○, WT. The data are from a single experiment.

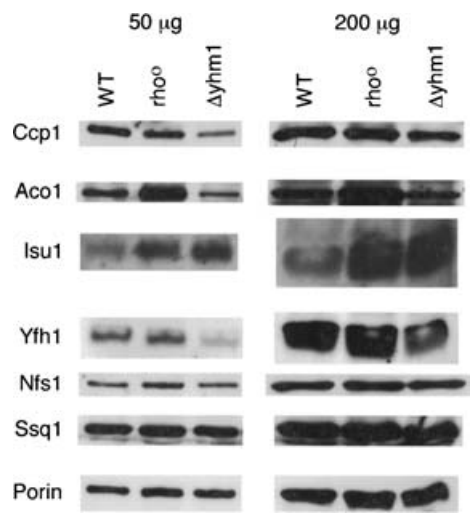

Figure 7 Protein levels in mitochondria from wild-type, rho° and *Δyhm1* mutants

Total mitochondrial protein, 50 or 200 μg, from BY4741 (wild-type), rho° or *Δyhm1* stains were separated by SDS/PAGE (13 % gel). After transfer to nitrocellulose, proteins were immunoblotted with the indicated antibodies. Antibodies directed against cytochrome *c* peroxidase (Ccp1p), aconitase (Aco1p), Isu1p, Yfh1p, Nfs1p, Ssq1p and porin were tested.

Family members have been implicated in the transport of varied substrates into and out of mitochondria [44] and, therefore, we reasoned that such transporters of this family with undefined substrates might influence iron homoeostasis. We found that the *Δyhm1* mutant of yeast, lacking one of these carriers, exhibited abnormally high iron uptake activities and misregulation of the high-affinity iron uptake systems. Iron taken up into the mutant cells rapidly accumulated in mitochondria, leaving the cytoplasm relatively iron-depleted.

We cannot say with certainty if these effects are direct or indirect. In the general scheme of cellular iron metabolism, iron must enter eukaryotic cells via specific permeases and then traverse cytoplasm, and external and internal mitochondrial membranes. Within mitochondria, critical transformations occur, creating haem and Fe–S clusters, and other biologically important forms of iron may also be made here. Subsequently, iron in various forms must exit mitochondria to reach structural and regulatory apoproteins in different extra-mitochondrial locations. Yhm1p in the mitochondrial inner membrane might directly transport iron from mitochondria to cytoplasm as haem, Fe–S or other form. Alternatively, Yhm1p might influence iron uptake and distribution indirectly, by transport of molecules that regulate these functions.

Many features of the *Δyhm1* mutant resemble features of Fe–S cluster assembly mutants. These mutants are deficient in mitochondrial proteins implicated in Fe–S cluster assembly. A large body of work has led to identification of more than 12 complementation groups of yeast mutants [43]. These mutants exhibit inappropriate activation of ferric reductase and ferrous transport [6], similar to *Δyhm1* mutants. The effects are mediated by *AFT1*, the sensor regulator responsible for transducing iron signals into regulated gene expression. Similarly, the misregulated high-affinity iron uptake in *Δyhm1* mutants was *AFT1* dependent and abrogated by *AFT1* deletion. Within the cells of Fe–S

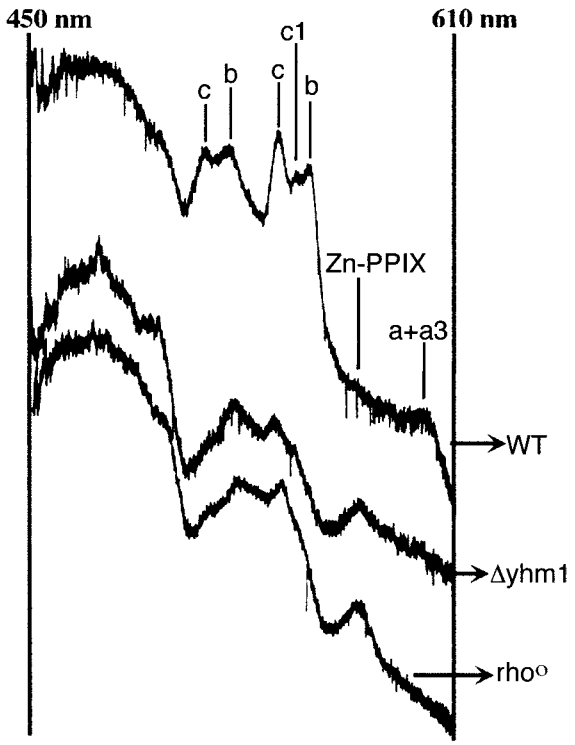

Figure 8 Cytochrome spectra

Low-temperature spectra on whole cell paste (WT, *Δyhm1* and rho°) grown in glucose were measured. *b* and *c* type cytochrome peaks are labelled. Zn-PPIX denotes absorption from zinc PP. Absorbance of the major peaks are $c + c1_{\beta}$ (509 nm), b_{β} (518 nm), c_{α} (546 nm), $c1_{\alpha}$ (552 nm), b_{α} (558 nm), Zn-PPIX (587 nm) and $a + a3$ (598 nm).

cluster assembly mutants, iron distribution shows abnormal accumulations in mitochondria and relative depletion in cytoplasm, also similar to *Δyhm1* mutants. Finally, iron accumulation in Fe–S cluster assembly mutants has been linked to mtDNA damage and loss. The proposed mechanism involves generation of oxygen intermediates such as hydrogen peroxide, which in turn produce reactive radicals in the presence of iron (Fenton chemistry) that damage DNA [45,46]. Such a mechanism might also be operative here, with iron accumulation in *Δyhm1* mitochondria producing toxic-free radicals, DNA damage and finally complete loss of mtDNA. A prior characterization of the *Δyhm1* phenotype did not observe mtDNA instability, although this difference may derive from genetic background effects [34].

The *Δyhm1* mutant did not phenocopy the Fe–S cluster assembly mutants entirely. As distinguished from mutants involved in Fe–S cluster assembly, Fe–S cluster protein activities were inconsistently affected in *Δyhm1* mutants. In *Δyhm1* mutants, decreases in aconitase but increases in succinate dehydrogenase activities were observed compared with the rho° control strain. Isopropylmalate dehydrogenase activity, dependent on the formation of an Fe–S cluster on the cytoplasmic protein Leu1p, was moderately decreased in the mutant compared with the rho° control. A virtual total deficiency of this enzyme was used to demonstrate a role for the Atm1p transporter in mediating export of a key component for cytoplasmic Fe–S cluster synthesis [7]. Disparate effects of the *Δyhm1* mutation on proteins mediating Fe–S cluster assembly were noted. Isu1p was increased, whereas Yfh1p was decreased. Nfs1p and Ssq1p were unchanged.

Effects on haem in the *Δyhm1* strain was also observed. Haem synthesis in isolated mitochondria measured from endogenous metals and exogenous porphyrins was decreased, despite the marked increase in iron within the organelle. Thus iron accumulating in the *Δyhm1* mutant was not fully available for use in haem synthesis. The defect here was much less severe when compared with that in frataxin mutants, in which haem synthesis from endogenous iron was virtually undetectable owing to a block in delivery of iron to ferrochelatase in the mitochondrial matrix [32]. The rho° strain showed marked deficiencies in cytochromes, making the specific effects of *Δyhm1* difficult to extrapolate. In *Δyhm1* mutants, cytochrome *c* peroxidase, a haem protein of the mitochondrial intermembrane space, was decreased further compared with the rho°.

Recent work has implicated the MCPs, Mrs3p and Mrs4p, in transport of iron into mitochondria. The double mutant in *MRS3* and *MRS4* (*Δmrs3/4*) abrogated mitochondrial iron accumulation of the *Δyfh1* mutant [20]. Studies using isolated mitochondria demonstrated a direct role for the corresponding proteins in iron transport and delivery for haem and Fe–S cluster formation in mitochondria [47]. Future work on Yhm1p will seek to address whether it is an iron transporter or transporter of a substrate that indirectly influences iron metabolism.

We thank Dr D. Pain for the gift of antibodies to cytochrome *c* peroxidase and for many helpful discussions. We also thank Dr G. B. Kohlhaw (Professor Emeritus, Purdue University and Indiana University Medical School) for helpful advice with the isopropylmalate isomerase assay. We are grateful to Dr Erfei Bi for the use of his microscope. This work was supported by grants from the National Institutes of Health Grant DK53953 (to A. D.) and from the French Ministère de la Recherche (Programme de Recherche Fondamentales en Microbiologie, Maladies Infectieuses et Parasitaires and Réseau Infection Fongique) and from the Association pour la Recherche sur le Cancer ARC 5439 (to E. L.).

REFERENCES

1 Brittenham, G. (2000) Disorders of iron metabolism: iron deficiency and overload. In Hematology, Basic Principles and Practice (Hoffman, R., Benz, E., Shattil, S., Furie, B., Cohen, H., Silberstein, L. and McGlave, P., eds.), pp. 397–428, Churchill Livingstone, New York
2 Dailey, H. A. (2002) Terminal steps of haem biosynthesis. Biochem. Soc. Trans. **30**, 590–595
3 Labbe-Bois, R. and Camadro, J.-M. (1994) Ferrochelatase in *Saccharomyces cerevisiae*. In Metal Ions in Fungi (Winkelmann, G. and Winge, D. R., eds.), pp. 413–454, Marcel Dekker, New York
4 Craig, E. A., Voisine, C. and Schilke, B. (1999) Mitochondrial iron metabolism in the yeast *Saccharomyces cerevisiae*. Biol. Chem. **380**, 1167–1173
5 Winzeler, E. A., Shoemaker, D. D., Astromoff, A., Liang, H., Anderson, K., Andre, B., Bangham, R., Benito, R., Boeke, J. D., Bussey, H. et al. (1999) Functional characterization of the *S. cerevisiae* genome by gene deletion and parallel analysis. Science **285**, 901–906
6 Li, J., Kogan, M., Knight, S. A. B., Pain, D. and Dancis, A. (1999) Yeast mitochondrial protein, Nfs1p, coordinately regulates iron–sulfur cluster proteins, cellular iron uptake, and iron distribution. J. Biol. Chem. **274**, 33025–33034
7 Kispal, G., Csere, P., Prohl, C. and Lill, R. (1999) The mitochondrial proteins Atm1p and Nfs1p are essential for biogenesis of cytosolic Fe/S proteins. EMBO J. **18**, 3981–3989
8 Knight, S. A. B., Sepuri, N. B. V., Pain, D. and Dancis, A. (1998) Mt-Hsp70 homolog, Ssc2p, required for maturation of yeast frataxin and mitochondrial iron homeostasis. J. Biol. Chem. **273**, 18389–18393
9 Kim, R., Saxena, S., Gordon, D. M., Pain, D. and Dancis, A. (2001) J-domain protein, Jac1p, of yeast mitochondria required for iron homeostasis and activity of Fe–S cluster proteins. J. Biol. Chem. **276**, 17524–17532
10 Garland, S. A., Hoff, K., Vickery, L. E. and Culotta, V. C. (1999) *Saccharomyces cerevisiae* ISU1 and ISU2: members of a well-conserved gene family for iron–sulfur cluster assembly. J. Mol. Biol. **294**, 897–907
11 Kaut, A., Lange, H., Diekert, K., Kispal, G. and Lill, R. (2000) Isa1p is a component of the mitochondrial machinery for maturation of cellular iron–sulfur proteins and requires conserved cysteine residues for function. J. Biol. Chem. **275**, 15955–15961
12 Li, J., Saxena, S., Pain, D. and Dancis, A. (2001) Adrenodoxin reductase homolog (Arh1p) of yeast mitochondria required for iron homeostasis. J. Biol. Chem. **276**, 1503–1509

13 Belenkiy, R., Haefele, A., Eisen, M. B. and Wohlrab, H. (2000) The yeast mitochondrial transport proteins: new sequences and consensus residues, lack of direct relation between consensus residues and transmembrane helices, expression patterns of the transport protein genes, and protein–protein interactions with other proteins. Biochim. Biophys. Acta **1467**, 207–218
14 Palmieri, L., Rottensteiner, H., Girzalsky, W., Scarcia, P., Palmieri, F. and Erdmann, R. (2001) Identification and functional reconstitution of the yeast peroxisomal adenine nucleotide transporter. EMBO J. **20**, 5049–5059
15 Dyall, S. D., Koehler, C. M., Delgadillo-Correa, M. G., Bradley, P. J., Plumper, E., Leuenaberger, D., Turck, C. W. and Johnson, P. J. (2000) Presence of a member of the mitochondrial carrier family in hydrogenosomes: conservation of membrane targeting pathways between hydrogenosomes and mitochondria. Mol. Cell. Biol. **20**, 2488–2497
16 Sullivan, T. D. and Kaneko, Y. (1995) The maize brittle 1 gene encodes amyloplast membrane polypeptides. Planta **196**, 477–484
17 Kunji, E. R. S. and Harding, M. (2003) Projection structure of the actractyloside-inhibited mitochondrial ADP/ATP carrier of *Saccharomyces cerevisiae*. J. Biol. Chem. **278**, 36985–36988
18 Palmieri, L., De Marco, V., Iacobazzi, V., Palmieri, F., Runswick, M. J. and Walker, J. E. (1997) Identification of the yeast ARG-11 gene as a mitochondrial ornithine carrier involved in arginine biosynthesis. FEBS Lett. **410**, 447–451
19 Prohl, C., Pelzer, W., Diekert, K., Kmita, H., Bedekovics, T., Kispal, G. and Lill, R. (2001) The yeast mitochondrial carrier Leu5p and its human homologue Graves' disease protein are required for accumulation of coenzyme A in the matrix. Mol. Cell. Biol. **21**, 1089–1097
20 Foury, F. and Roganti, T. (2002) Deletion of the mitochondrial carrier genes MRS3 and MRS4 suppresses mitochondrial iron accumulation in a yeast frataxin-deficient strain. J. Biol. Chem. **277**, 24475–24483
21 Muhlenhoff, U., Stadler, J. A., Richhardt, N., Seubert, A., Eickhorst, T., Schweyen, R. J., Lill, R. and Wiesenberger, G. (2003) A specific role of the yeast mitochondrial carriers Mrs3/4p in mitochondrial iron acquisition under iron-limiting conditions. J. Biol. Chem. **278**, 40612–40620
22 Luk, E., Carroll, M., Baker, M. and Culotta, V. C. (2003) Manganese activation of superoxide dismutase 2 in *Saccharomyces cerevisiae* requires MTM1, a member of the mitochondrial carrier family. Proc. Natl. Acad. Sci. U.S.A. **100**, 10353–10357
23 Wach, A., Brachat, A., Rebischung, C., Steiner, S., Pokorni, K., te Heesen, S. and Philippsen, P. (1998) PCR-based gene targeting in *Saccharomyces cerevisiae*. In Methods in Microbiology, vol. 26 (Brown, A. J. and Tuite, M. F., eds.), pp. 67–81, Academic Press, San Diego
24 Fox, T. D., Folley, L. S., Mulero, J. J., McMullin, T. W., Thorsness, P. E., Hedin, L. O. and Costanzo, M. C. (1991) Analysis and manipulation of yeast mitochondrial genes. Methods Enzymol. **194**, 149–165
25 Sherman, F., Fink, G. R. and Hicks, J. B. (1986) Laboratory Course Manual for Methods in Yeast Genetics, Cold Spring Harbor Laboratory Press, Cold Spring Harbor, NY
26 Lesuisse, E., Knight, S. A. B., Camadro, J. M. and Dancis, A. (2002) Siderophore uptake by *Candida albicans*: effect of serum treatment and comparison with *Saccharomyces cerevisiae*. Yeast **19**, 329–340
27 Kennedy, M. C., Emptage, M. H., Dreyer, J. L. and Beinert, H. (1983) The role of iron in the activation–inactivation of aconitase. J. Biol. Chem. **258**, 11098–11105
28 Munujos, P., Coll-Canti, J., Gonzalez-Sastre, F. and Gella, F. J. (1993) Assay of succinate dehydrogenase activity by a colorimetric-continuous method using iodonitrotetrazolium chloride as electron acceptor. Anal. Biochem. **212**, 506–509
29 Kohlhaw, G. B. (1988) Isopropylmalate dehydratase from yeast. Methods Enzymol. **166**, 423–429
30 Gordon, D. M., Kogan, M., Knight, S. A., Dancis, A. and Pain, D. (2001) Distinct roles for two N-terminal cleaved domains in mitochondrial import of the yeast frataxin homolog, Yfh1p. Hum. Mol. Genet. **10**, 259–269
31 Murakami, H., Pain, D. and Blobel, G. (1988) 70-kD heat shock-related protein is one of at least two distinct cytosolic factors stimulating protein import into mitochondria. J. Cell Biol. **107**, 2051–2057
32 Lesuisse, E., Santos, R., Matzanke, B. F., Knight, S. A., Camadro, J.-M. and Dancis, A. (2003) Iron use for haeme synthesis is under control of the yeast frataxin homologue (Yfh1). Hum. Mol. Genet. **12**, 879–889
33 Camadro, J.-M., Chambon, H., Jolles, J. and Labbe, P. (1986) Purification and properties of coproporphyrinogen oxidase from the yeast *Saccharomyces cerevisiae*. Eur. J. Biochem. **156**, 579–587
34 Kao, L. R., Megraw, T. L. and Chae, C. B. (1996) SHM1: a multicopy suppressor of a temperature-sensitive null mutation in the HMG1-like abf2 gene. Yeast **12**, 1239–1250
35 Yamaguchi-Iwai, Y., Dancis, A. and Klausner, R. D. (1995) AFT1: a mediator of iron regulated transcriptional control in *Saccharomyces cerevisiae*. EMBO J. **14**, 1231–1239
36 Blaiseau, P. L., Lesuisse, E. and Camadro, J. M. (2001) Aft2p, a novel iron-regulated transcription activator that modulates, with aft1p, intracellular iron use and resistance to oxidative stress in yeast. J. Biol. Chem. **276**, 34221–34226
37 Rutherford, J. C., Jaron, S., Ray, E., Brown, P. O. and Winge, D. R. (2001) A second iron-regulatory system in yeast independent of Aft1p. Proc. Natl. Acad. Sci. U.S.A. **98**, 14322–14327
38 Lesuisse, E., Blaiseau, P. L., Dancis, A. and Camadro, J. M. (2001) Siderophore uptake and use by the yeast *Saccharomyces cerevisiae*. Microbiology **147**, 289–298
39 Yun, C. W., Ferea, T., Rashford, J., Ardon, O., Brown, P. O., Botstein, D., Kaplan, J. and Philpott, C. C. (2000) Desferrioxamine-mediated iron uptake in *Saccharomyces cerevisiae*. Evidence for two pathways of iron uptake. J. Biol. Chem. **275**, 10709–10715
40 Yun, C. W., Tiedeman, J. S., Moore, R. E. and Philpott, C. C. (2000) Siderophore-iron uptake in *Saccharomyces cerevisiae*. Identification of ferrichrome and fusarinine transporters. J. Biol. Chem. **275**, 16354–16359
41 Esser, K., Tursun, B., Ingenhoven, M., Michaelis, G. and Pratje, E. (2002) A novel two-step mechanism for removal of a mitochondrial signal sequence involves the mAAA complex and the putative rhomboid protease Pcp1. J. Mol. Biol. **323**, 835–843
42 Askwith, C. and Kaplan, J. (1998) Iron and copper transport in yeast and its relevance to human disease. Trends Biochem. Sci. **23**, 135–138
43 Lill, R. and Kispal, G. (2000) Maturation of cellular Fe–S proteins: an essential function of mitochondria. Trends Biochem. Sci. **25**, 352–356
44 Palmieri, L., Runswick, M. J., Fiermonte, G., Walker, J. E. and Palmieri, F. (2000) Yeast mitochondrial carriers: bacterial expression, biochemical identification and metabolic significance. J. Bioenerg. Biomembr. **32**, 67–77
45 Chen, O. S. and Kaplan, J. (2000) CCC1 suppresses mitochondrial damage in the yeast model of Friedreich's ataxia by limiting mitochondrial iron accumulation. J. Biol. Chem. **275**, 7626–7632
46 Karthikeyan, G., Lewis, L. K. and Resnick, M. A. (2002) The mitochondrial protein frataxin prevents nuclear damage. Hum. Mol. Genet. **11**, 1351–1362
47 Muhlenhoff, U., Stadler, J. A., Richhardt, N., Seubert, A., Eickhorst, T., Schweyen, R. J., Lill, R. and Wiesenberger, G. (2003) A specific role of the yeast mitochondrial carriers MRS3/4p in mitochondrial iron acquisition under iron-limiting conditions. J. Biol. Chem. **278**, 40612–40620
48 Dancis, A., Yuan, D. S., Haile, D., Askwith, C., Eide, D., Moehle, C., Kaplan, J. and Klausner, R. D. (1994) Molecular characterization of a copper transport protein in *S. cerevisiae*: an unexpected role for copper in iron transport. Cell (Cambridge, Mass.) **76**, 393–402

Received 11 September 2003/13 November 2003; accepted 20 November 2003
Published as BJ Immediate Publication 20 November 2003, DOI 10.1042/BJ20031387